ISSN 1068-3356, Bulletin of the Lebedev Physics Institute, 2024, Vol. 51, Suppl. 7, pp. S594–S601. © Allerton Press, Inc., 2024.
Russian Text © The Author(s), 2024, published in Kvantovaya Elektronika, 2024, Vol. 54, No. 4, pp. 249–254.

## APPLICATIONS OF LASERS AND OTHER QUESTIONS OF QUANTUM ELECTRONICS

# Control of Dimensional and Optical Properties of Laser-Synthesized TiN Nanoparticles for Biomedical Applications

**V. S. Chernyakova[a], G. V. Tikhonovskii[a,*], A. P. Satina[a], I. V. Sozaev[a], M. S. Savinov[a], P. V. Shakhov[a], D. I. Tselikov[a], A. A. Popov[a], A. A. Fronya[b], I. N. Zavestovskaya[c], S. M. Klimentov[a], and A. V. Kabashin[d]**

[a]*National Research Nuclear University MEPhI, Engineering Physics Institute of Biomedicine, Moscow, 115409 Russia*
[b]*Lebedev Physical Institute of the Russian Academy of Sciences, Moscow, 119991 Russia*
[c]*National Research Center Kurchatov Institute, Moscow, 123182 Russia*
[d]*LP3, Aix Marseille University, CNRS, Marseille, 13288 France*
**e-mail: gtikhonowski@gmail.com*

Received July 15, 2024; revised August 1, 2024; accepted August 1, 2024

**Abstract**—The dimensional and optical properties of nanomaterials largely determine the prospects of their application in biomedicine. We have studied the feasibility of controlling the dimensional and optical characteristics of laser-synthesized titanium nitride (TiN) nanoparticles (NP) using various liquid media (water, isopropanol, acetone, or acetonitrile) and laser focusing parameters and energy. Laser ablation of the TiN target in all solvents resulted in the formation of spherical NPs with the mode and half-width of the size distribution dependent on the type of liquid. We show that the use of organic solvents can produce NPs with higher coefficients of mass extinction (up to 35.2 L $cm^{-1}$ $g^{-1}$) and of photothermal conversion (up to 69%) in the window of relative biotissue transparency for aqueous medium. It is also demonstrated that the mode and half-width of the TiN NP size distribution decreases as the distance from the lens to the target surface increases or laser radiation energy decreases. These findings form a quantitative basis for developing laser-synthesized TiN NPs with controlled properties and they also prove their high potential for applications in biomedicine.

**Keywords:** titanium nitride, nanoparticles, laser ablation in liquid, biomedicine, dimensional properties, optical properties

**DOI:** 10.3103/S106833562460181X

## 1. INTRODUCTION

Despite the long and successful history of progress in classical oncologic therapies and diagnostics, these approaches still have many limitations in clinical practice [1]. Nanotechnology has become an indispensable innovative tool for the development of modern biomedicine due to a wide range of unique physical and chemical properties inherent in NPs [2, 3]. Strong photoabsorption in the window of relative transparency of biotissues (650 to 950 nm) by plasmonic nanostructures caused rapid growth of photothermal therapy (PTT), an innovative method of cancer control which showed promising results in the treatment of prostate cancer (method efficiency is 94%) [4]. At the same time, the use of NPs with a relatively low work function can be applied successfully to sensibilization of the most promising methods of radiation therapy, for example, proton radiation [5]. In addition, the small size of NPs additionally facilitates their higher localization in target areas due to passive accumulation and retention during circulation in the bloodstream, which can significantly enhance the therapeutic efficacy of PTT and of proton therapy [4, 5].

The dimensional characteristics of nanomaterials affect their colloidal stability, optical properties, efficiency of cell internalization, and duration of circulation in the bloodstream with the optimal size for in vivo biomedical applications being 50 nm [6]. Classical photoabsorbing NPs are based on noble metals (Pd, Ag, Pt, and Au). However, these nanostructures usually demonstrate plasmonic absorption only in the UV and visible spectral regions, which significantly limits their application in the therapy of deep-seated tumors. Another solution is to use biocompatible alternative plasmonic materials such as Group IV transition metal nitrides (TiN, ZrN, HfN) or layered nanostructures based on transition metal chalco-

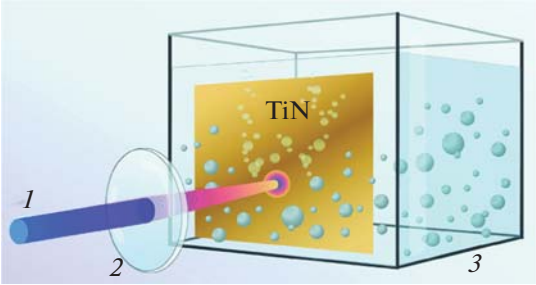


**Fig. 1.** Schematic representation of the experimental setup for laser synthesis of TiN nanoparticles: (*1*) fs Yb:KGW laser, (*2*) focusing lens, (*3*) ablation cuvette with TiN target.

genides ($MoS_2$, $WS_2$) [7–9]. Their unique optical properties cause increased absorption in a wide spectral range even with strictly spherical morphology. One of the most promising of the presented materials is TiN whose pronounced therapeutic effect and low toxicity have already been demonstrated in a series of biological experiments [10–12]. In addition, TiN has a lower work function, which can be used for sensibilization of proton therapy [13]. However, the description of methods for controlling the dimensional and optical properties of TiN NPs has not been sufficiently covered in the literature so far.

The traditional methods for producing TiN NPs are based on chemical synthesis approaches often using toxic precursors and multistep procedures to initiate reactions [14]. Another approach based on plasma methods is limited by the low colloidal stability of NPs and by the wide spread of their dimensional and morphological characteristics [15]. In this context, pulsed laser ablation in liquid (PLAL), which can produce stable ultrapure NPs with controlled physicochemical properties, looks like an attractive alternative to classical methods [16–20]. The versatility, ease of performance, and high productivity of PLAL make the method popular for a wide range of applications, including the most urgent challenges in biomedicine [21–24].

This paper investigates the dependences on the type of liquid medium of mass and photothermal conversion coefficients in the region of relative transparency of biological tissues and of the mode and halfwidth of the size distribution of laser-synthesized TiN NPs. Special attention is paid to studying the dependence of the dimensional properties of NPs on the focusing parameters and laser radiation energy. It is shown that the use of liquids with high oxygen content in the initial composition (water or isopropanol) leads to the formation of TiN NPs with lower mass extinction and photothermal conversion for acetone and acetonitrile. At the same time, organic solvents additionally help to reduce the mode and halfwidth of the size distribution for synthesis in aqueous medium. Moreover, higher distance from the focusing lens to the target surface and lower laser pulse energy can also result in a controlled reduction of dimensional characteristics.

## 2. MATERIALS AND METHODS

### *2.1. TiN NP synthesis*

TiN nanoparticles were synthesized by the femtosecond (fs) PLAL method (Fig. 1). For this purpose, the target of crystalline TiN (Girmet, Russia; 99.9% purity) was fixed vertically in a glass cuvette filled with 10 ml of liquid (water, isopropanol, acetone, or acetonitrile). A Yb:KGW TETA-20 fs laser (Avesta, Russia; 1030 nm, 250 fs, 20 μJ, 200 kHz) was used as a radiation source. The radiation was focused on the target surface using an F-Theta flat-field lens (Thorlabs, United States) with a focal length of 100 mm. In order to increase the synthesis productivity, laser radiation was moved along the target surface with an LScan galvanometry scanner (Ateco-TM, Russia) at 2 m/s (50 μm spot size, 80% overlap) and the thickness of the liquid layer in front of the target was reduced to the optimal 3 mm [25]. The synthesis procedure lasted 10 min.

### *2.2. TiN NP characterization*

The hydrodynamic size distribution of the NPs thus produced was measured by dynamic light scattering (DLS) (Zetasizer, Malvern Instruments, United Kingdom). The dimensional and morphological properties of TiN NPs were characterized with scanning electron microscopy (SEM) MALA 3 (Tescan, Czech Republic) at an accelerating voltage of 25 kV. Optical extinction spectra were measured in the spec-

tral range of 350 to 1100 nm by an ML122 spectrophotometer (SOL Instruments, Belarus). The NP concentration was estimated by gravimetric method measuring the mass of a dried sample of fixed volume on high-precision scales (±0.01 mg). To evaluate the photothermal properties of NPs, TiN was exposed in a glass cuvette (the optical path length being 10 mm) to constant laser radiation (830 nm, 716 mW, beam diameter 2 mm). The concentration of the samples was 0.075 g/L. The colloidal solution was homogenized with a magnetic stirrer to ensure homogeneous heating of the entire liquid volume throughout the experiment. Temperature measurements were made using a FLLR C3 thermal imager (FLIR Systems, United States). The photothermal conversion efficiency (η) of NPs was calculated by the method developed in [26]:

$$\eta = \frac{\Delta T_{max} m_{liq} C_{liq} B}{I_0 - I_{pass}} 100\%,$$

where $\Delta T_{max}$ is maximum temperature difference between the NP solution and ambient temperature; $m_{liq}$ and $C_{liq}$ are mass and specific heat capacity of the liquid medium, respectively; $B$ is the time constant defined as the slope coefficient of the cooling time dependence on the logarithm of the $\Delta T_{max}/\Delta T(t)$ ratio; $I_0$ is the initial radiation power; and $I_{pass}$ is power after passing the cuvette with the solution.

## 3. RESULTS AND DISCUSSION

All colloidal solutions of TiN NPs produced by laser ablation in various liquid media demonstrated increased extinction in the region of relative transparency of biological tissues (Fig. 2a). However, the spectral position of the extinction maximum depended on the type of liquid in which NPs were obtained. The shift of the peak was observed in the range of 640 to 670 nm including 640 nm in isopropanol, 660 nm in water, 665 nm in acetonitrile, and 670 nm in acetone. The extinction maximum variation can be related both to the formation of an oxide or carbon-containing shell on the NP surface and to their dimensional properties [27]. The highest mass extinction coefficient in the biotissue transparency window was observed for TiN NPs synthesized in acetone (35.2 L $cm^{-1}$ $g^{-1}$), which exceeds typical values for $Fe_3O_4$ (15.1 L $cm^{-1}$ $g^{-1}$), $Mo_2C$ (18.0 L $cm^{-1}$ $g^{-1}$), $WS_2$ (23.8 L $cm^{-1}$ $g^{-1}$), and $MoS_2$ (28.4 L $cm^{-1}$ $g^{-1}$) [28–31] while similar values for acetonitrile, isopropanol and water were 28.4, 25.4, and 17.8 L $cm^{-1}$ $g^{-1}$, respectively. It is also worth noting that extinction in the long-wavelength region can be increased by an input of scattering from relatively large nanoparticles. A similar correlation is observed when comparing the spectral profiles of mass extinction and dimensional characteristics of NPs studied by the DLS method (Fig. 2b). The largest mode and half-width of the size distribution (60 ± 40 nm) were observed for an aqueous solution of TiN NPs, which had a pronounced extinction shoulder in the long-wave part of the spectrum. The maximum diameter of TiN NPs produced in water reached 250 nm. On the other hand, laser ablation in organic solvents led to a pronounced decrease in the NP dimensional characteristics including 40 ± 22, 35 ± 24, and 14 ± 8 nm for isopropanol, acetone, and acetonitrile, respectively. At the same time, there was a bimodal distribution with a second mode of around 35 nm and a half-width of 20 nm for TiN NPs synthesized in acetonitrile. It should be noted that the use of organic solvents for the synthesis does not limit the future application of NPs in biomedicine [12]. Nanomaterials can be re-dispersed if necessary into biologically relevant liquid media by adding another centrifugation step.

The dimensional and morphological characteristics of the investigated nanoparticles were additionally analyzed by SEM (Fig. 3). The size distributions of laser-synthesized TiN NPs were obtained by analyzing SEM images in the ImageJ software environment using circle approximation. The final distributions were of lognormal nature and were based on measurements of diameters from 200 to 300 TiN PMs

It can be seen from obtained data that all synthesized NPs have morphology close to spherical. And the results of measurements of dimensional characteristics are in high correlation with the DLS results: 38 ± 28, 32 ± 27, and 28 ± 23 nm for water (Fig. 3a), isopropanol (Fig. 3b), and acetone (Fig. 3c), respectively. The SEM-image analysis of TiN NPs synthesized in acetonitrile (Fig. 3d) did not find pronounced bimodal size distribution with characteristics of 22 ± 19 nm, which is due to the specific features of DLS measurements.

This variation of the dimensional characteristics of nanomaterials synthesized in different organic solvents may be due to the formation of a carbon-containing matrix on the NP surface during laser-induced decomposition of liquid medium molecules limiting their growth, which is typical of pulsed laser ablation [17].

The photothermal activity of TiN NPs synthesized in various liquids was studied in addition (Fig. 4). The heating temperature profiles (Fig. 4a) are in high agreement with the results of mass extinction coefficient measurements. The highest temperature rise was observed for TiN NPs synthesized in acetone and

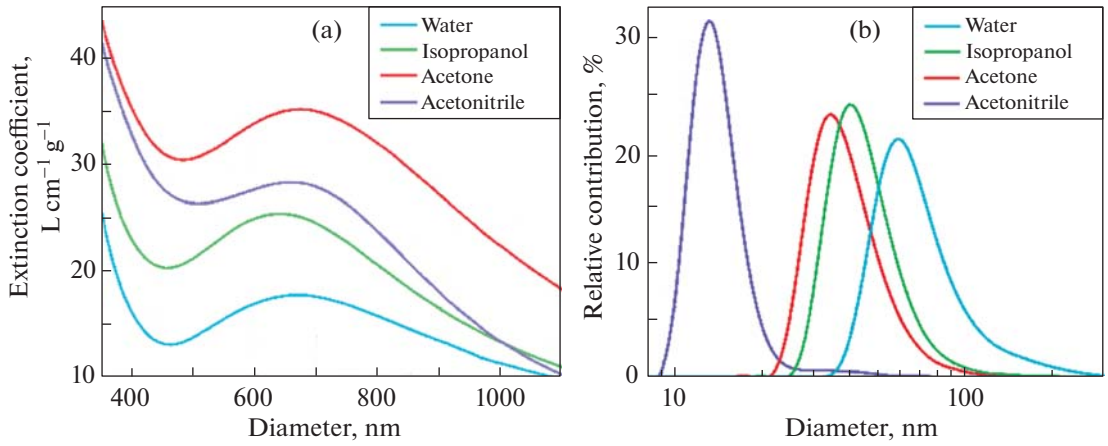


**Fig. 2.** (a) Mass extinction coefficient and (b) hydrodynamic size distribution of TiN NPs synthesized in different liquid media.

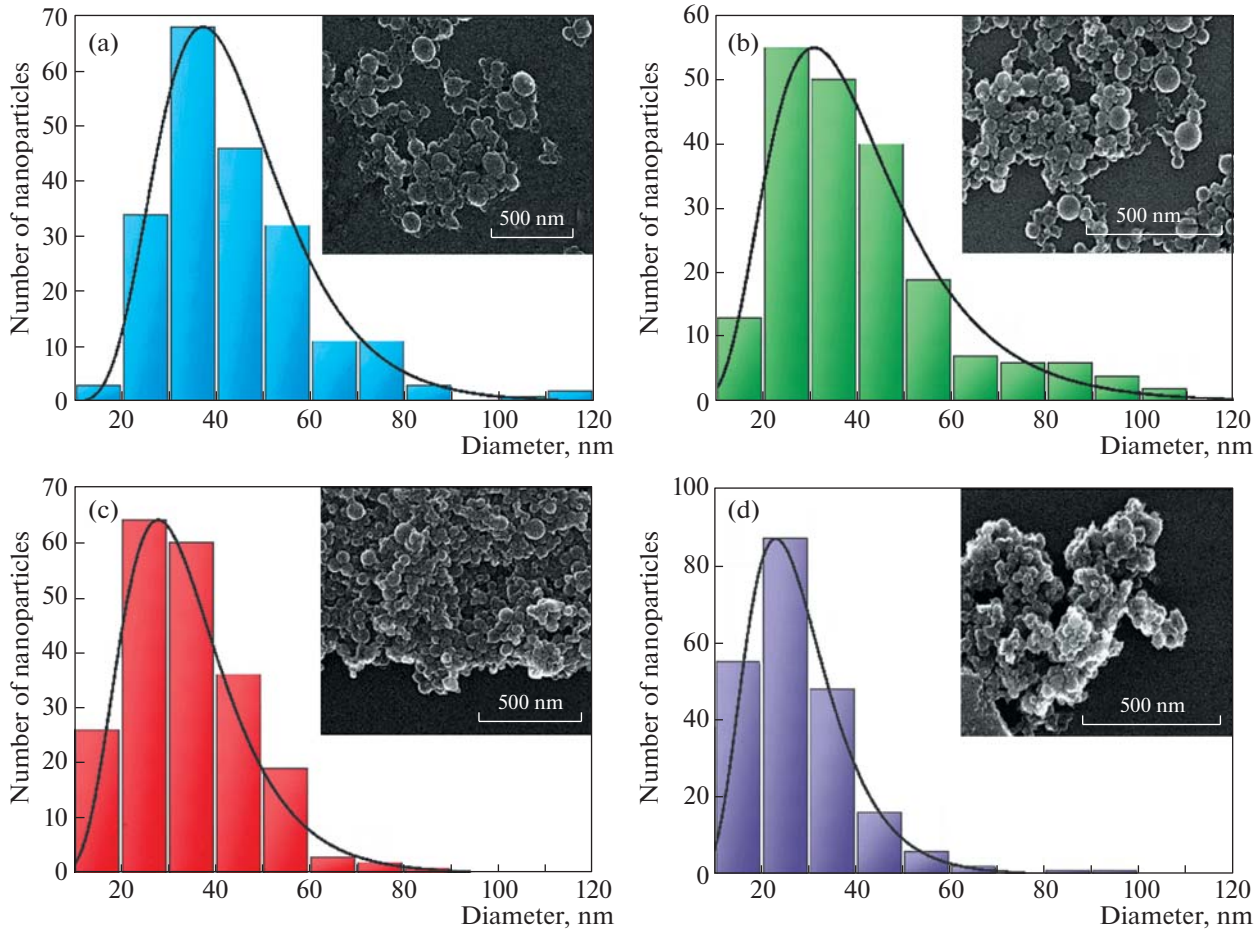


**Fig. 3.** Size distributions and SEM images of TiN NPs synthesized in (a) water, (b) isopropanol, (c) acetone, and (d) acetonitrile.

acetonitrile reaching approximately 30 and 29°C, respectively. At the same time, similar values for isopropanol and water were about 25 and 21°C, respectively. The heating rate was practically the same for all samples synthesized in organic solvents (Fig. 4b) reaching a maximum of 7.2°C/min followed by an exponential decline until thermodynamic equilibrium was established.

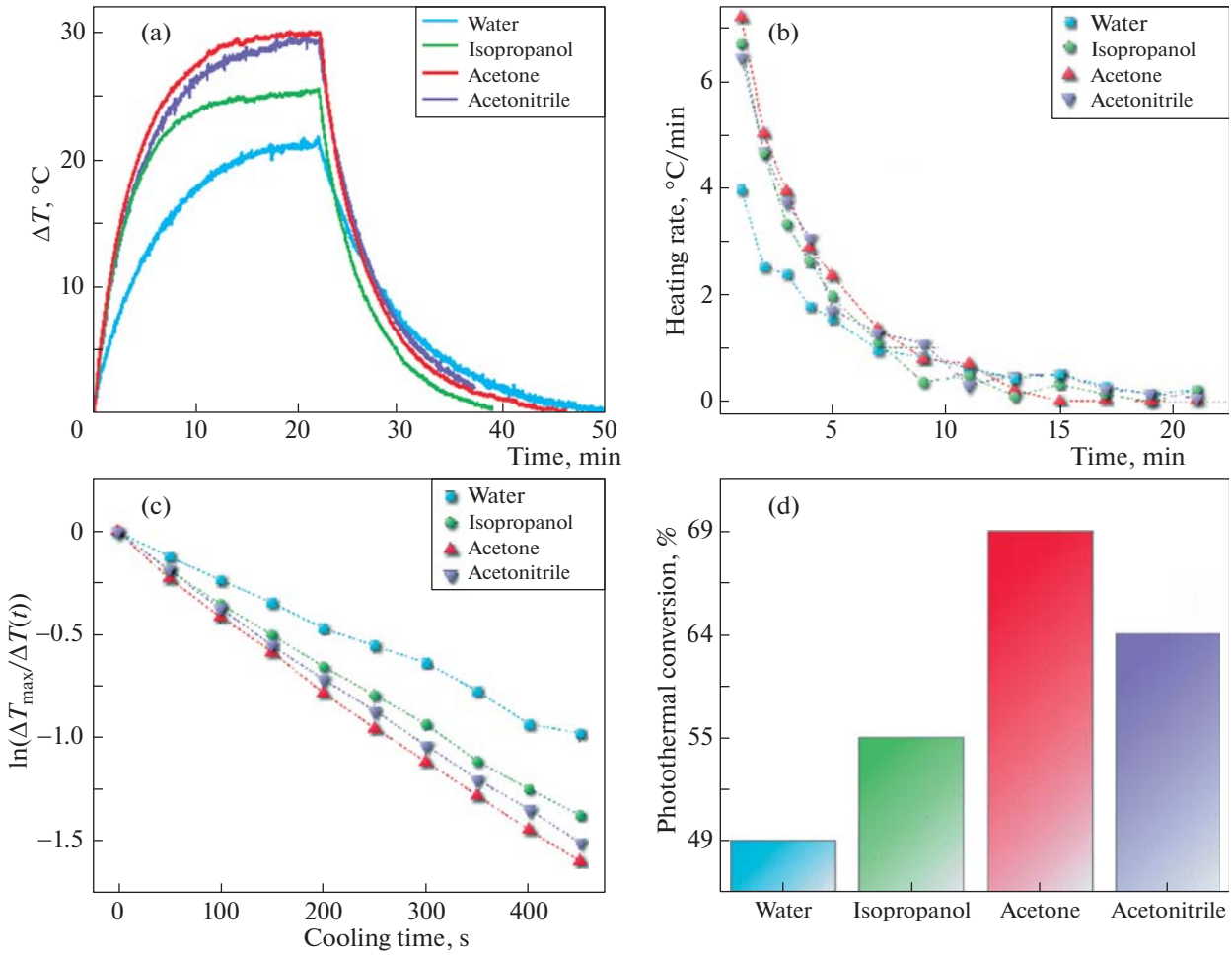


**Fig. 4.** (a) Heating temperature profile, (b) heating rate curve, (c) logarithmic cooling curve, and (d) photothermal conversion coefficient of TiN NPs synthesized in different fluids.

An analysis of the cooling profiles of colloidal solutions of TiN NPs (Fig. 4c) was used to determine the time constant $B$ required to calculate the photothermal conversion coefficient according to [26]. Final calculations allowed us to state that the highest photothermal conversion coefficient was observed for TiN NPs synthesized in acetone ($\eta = 69\%$), which exceeds these values for $MoSe_2$ ($\eta = 46\%$), Ge ($\eta = 44\%$), and $WS_2$ ($\eta = 43\%$). Similar values of $\eta$ for acetonitrile, isopropanol, and water were 64, 55, and 49%, respectively. These results fully agree with mass extinction coefficient measurements and heating temperature profiles.

The combination of optimal dimensional and optical characteristics of TiN NPs synthesized in acetone makes promising their further application for biomedicine. Then a detailed analysis of the strategy for controlling the dimensional properties and synthesis productivity was carried out exactly for this type of liquid. The productivity of fs-PLAL depends most of all on the focusing parameters, laser intensity, and the thickness of the liquid layer in front of the target [17]. At the same time, the propagation of ultrashort radiation in liquid media entails a number of nonlinear effects including the Kerr effect, self-focusing, and filamentation. Therefore, the position of the focal plane during PLAL is often determined experimentally by measuring the synthesis productivity according to the position of the focusing lens; in this case, the synthesis productivity directly correlates with the optical density (extinction) of the obtained samples (Fig. 5a).

Maximum productivity of laser-ablation synthesis of TiN NPs in acetone at a laser pulse energy of 20 μJ, repetition rate of 100 kHz and duration of 250 fs reaches 14.7 mg/h, which corresponds to the position of the focal plane, and decreases to 2.2 mg/h when shifted by 5 mm (Fig. 5b). At the same time, the synthesis productivity per pulse reached a maximum of 40.8 fg/pulse and dropped to 6.1 fg/pulse as it moved away from the focal plane. The extinction of the resulting solutions also tended to decrease with

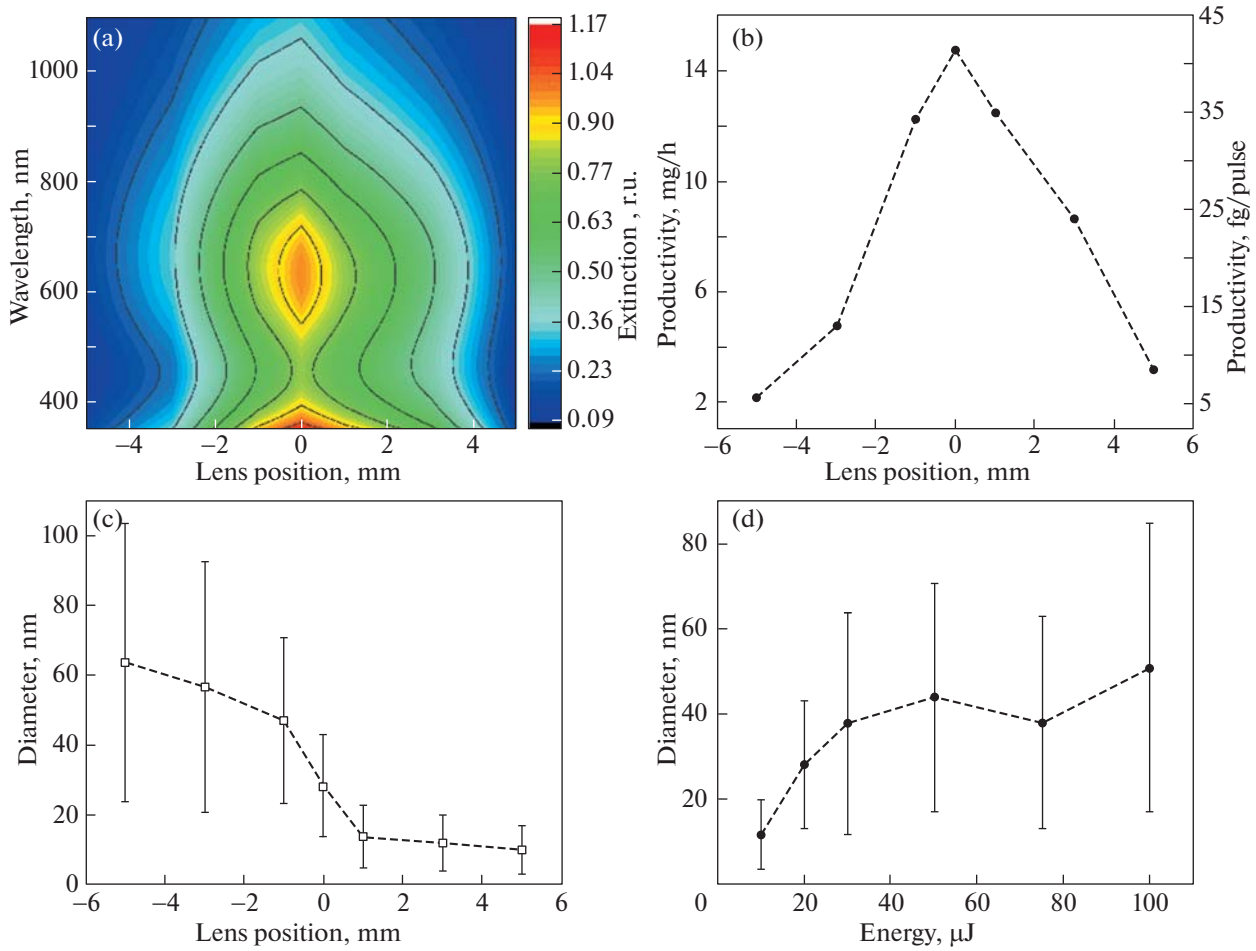


**Fig. 5.** (a) The dependences of the extinction spectra, (b) laser synthesis productivity, (c) mode (squares) and half-width (vertical lines) of the size distribution (DLS) on the lens position relative to the target surface at a pulse energy of 20 μJ and (d) the dependence of the mode and half-width of the size distribution on the laser pulse energy. The position of the maximum efficiency of laser synthesis is taken as the zero point.

distance from the focal position (Fig. 5a). However, any change in the distance between the focusing lens and the surface changed not only the synthesis productivity but also the dimensional characteristics of NPs (Fig. 5c). By varying this distance within 10 mm we can control the mode and half-width of the size distribution from $10 \pm 7$ nm to $64 \pm 40$ nm. An additional parameter that allows to control the dimensional characteristics of TiN NPs is the energy of laser pulses (Fig. 5d). Radiation energy variation in the range of 10 to 100 μJ can change the mode of distribution from 11 to 56 nm the half-width from 8 to 34 nm, respectively.

## 4. CONCLUSIONS

A quantitative method for controlling the dimensional and optical properties of laser-synthesized TiN NPs has been developed. Laser ablation of a TiN solid target is shown to be able to produce colloidal solutions of NPs in different liquid media with mass extinction coefficients of 17.8 L $cm^{-1}$ $g^{-1}$ (water), 25.4 L $cm^{-1}$ $g^{-1}$ (isopropanol), 28.4 L $cm^{-1}$ $g^{-1}$ (acetonitrile), and 35.2 L $cm^{-1}$ $g^{-1}$ (acetone). Changing the type of liquid medium allows additionally to control the dimensional characteristics of laser-synthesized TiN NPs from $14 \pm 8$ nm (acetonitrile) to $60 \pm 40$ nm (water) and the photothermal conversion coefficient from $\eta = 49\%$ (water) to $\eta = 69\%$ (acetone). Laser-synthesized TiN NPs produced in isopropanol, acetone, or acetonitrile have optimal dimensional and optical characteristics for applications in cancer theranostics. In addition, we have demonstrated an alternative possibility of controlling the dimensional characteristics by varying laser focusing parameters and energy. It is shown that by increasing the distance from the focusing lens to the target surface we can reduce the mode and half-width of the size distribution

from 64 ± 40 nm to 10 ± 7 nm with deviation from the focal plane by −5 mm and +5 mm, respectively. At the same time, as laser energy increases from 10 to 100 μJ, the mode and half-width of the distribution rise from 11 ± 8 nm to 56 ± 34 nm. These findings form a quantitative basis for creating laser-synthesized TiN NPs with controlled dimensional and optical properties and also prove their high potential for applications in biomedicine.

## ACKNOWLEDGMENTS

The authors are grateful for the provision of scientific infrastructure for research.

## FUNDING

This work was supported by the Ministry of Science and Higher Education of the Russian Federation under Agreement no. 075-15-2021-1347 (grant no. FSWU-2023-0070).

## CONFLICT OF INTEREST

The authors declare that they have no conflicts of interest.

## REFERENCES

1. Schaue, D. and McBride, W.H., *Nat. Rev. Clin. Oncol.,* 2015, vol. 12, p. 527.
2. Chaturvedi, V.K., Singh, A., Singh, V.K., and Singh, M.P., *Curr. Drug Metab.,* 2019, vol. 20, p. 416.
3. Kalyane, D., Raval, N., Maheshwari, R., Tambe, V., Kalia, K., and Tekade, R.K., *Mater. Sci. Eng. C,* 2019, vol. 98, p. 1252.
4. Rastinehad, A.R., Anastos, H., Wajswol, E., Winoker, J.S., Sfakianos, J.P., Doppalapudi, S.K., Carrick, M.R., Knauer, C.J., Taouli, B., Lewis, S.C., Tewari, A.K., Schwartz, J.A., Canfield, S.E., George, A.K., West, J.L., and Halas, N.J., *Proc. Natl. Acad. Sci.,* 2019, vol. 116, p. 18590.
5. Zwiehoff, S., Johny, J., Behrends, C., Landmann, A., Mentzel, F., Bäumer, C., Kröninger, K., Rehbock, C., Timmermann, B., and Barcikowski, S., *Small,* 2022, vol. 18, p. 2106383.
6. Hoshyar, N., Gray, S., Han, H., and Bao, G., *Nanomedicine,* 2016, vol. 11, p. 673.
7. Kim, S., Kim, J., Park, J., and Nam, J., *Adv. Mater.,* 2018, vol. 30, p. 1704528.
8. Karaballi, R.A., Esfahani Monfared, Y., and Dasog, M., *Langmuir,* 2020, vol. 36, p. 5058.
9. Tselikov, G.I., Ermolaev, G.A., Popov, A.A., Tikhonowski, G.V., Panova, D.A., Taradin, A.S., Vyshnevyy, A.A., Syuy, A.V., Klimentov, S.M., Novikov, S.M., Evlyukhin, A.B., Kabashin, A.V., Arsenin, A.V., Novoselov, K.S., and Volkov, V.S., *Proc. Natl. Acad. Sci.,* 2022, vol. 119, p. e2208830119.
10. Popov, A.A., Tselikov, G., Dumas, N., Berard, C., Metwally, K., Jones, N., Al-Kattan, A., Larrat, B., Braguer, D., Mensah, S., Da Silva, A., and Estève, M.-A., *Sci. Rep.,* 2019, vol. 9, p. 1194.
11. He, W., Ai, K., Jiang, C., Li, Y., Song, X., and Lu, L., *Biomaterials,* 2017, vol. 132, p. 37.
12. Zelepukin, I.V., Popov, A.A., Shipunova, V.O., Tikhonowski, G.V., Mirkasymov, A.B., Popova-Kuznetsova, E.A., Klimentov, S.M., Kabashin, A.V., and Deyev, S.M., *Mater. Sci. Eng. C,* 2021, vol. 120, p. 111717.
13. Ma, T., Jacobs, R., Booske, J., and Morgan, D., *J. Phys. Chem. C,* 2021, vol. 125, p. 17400.
14. Yang, X., Li, C., Yang, L., and Yan, Y., *J. Am. Ceram. Soc.,* 2003, vol. 86, p. 206.
15. Zhang, H., Li, F., and Jia, Q., *Ceram. Int.,* 2009, vol. 35, p. 1071.
16. Kabashin, A.V. and Meunier, M., *J. Phys. Conf. Ser.,* 2007, vol. 59, p. 354.
17. Zhang, D., Gökce, B., and Barcikowski, S., *Chem. Rev.,* 2017, vol. 117, p. 3990.
18. Fojtik, A. and Henglein, A., *Ber. Bunsen-Ges. Phys. Chem.,* 1993, vol. 97, p. 252.
19. Mafuné, F., Kohno, J., Takeda, Y., Kondow, T., and Sawabe, H., *J. Phys. Chem. B,* 2000, vol. 104, p. 9111.
20. Kabashin, A.V. and Meunier, M., *J. Appl. Phys.,* 2003, vol. 94, p. 7941.
21. Griaznova, O.Yu., Belyaev, I.B., Sogomonyan, A.S., Zelepukin, I.V., Tikhonowski, G.V., Popov, A.A., Komlev, A.S., Nikitin, P.I., Gorin, D.A., and Kabashin, A.V., *Pharmaceutics,* 2022, vol. 14, p. 994.
22. Bulmahn, J.C., Tikhonowski, G., Popov, A.A., Kuzmin, A., Klimentov, S.M., Kabashin, A.V., and Prasad, P.N., *Nanomaterials,* 2020, vol. 10, p. 1463.
23. Belyaev, I.B., Zelepukin, I.V., Kotelnikova, P.A., Tikhonowski, G.V., Popov, A.A., Kapitannikova, A.Yu., Barman, J., Kopylov, A.N., Bratashov, D.N., Prikhozhdenko, E.S., Kabashin, A.V., and Deyev, S.M., *Adv. Sci.,* 2024, vol. 11, p. 2307060.
24. Maldonado, M.E., Das, A., Gomes, A.S.L., Popov, A.A., Klimentov, S.M., and Kabashin, A.V., *Opt. Lett.,* 2020, vol. 45, p. 6695.

25. Barcikowski, S., et al., *Handbook of Laser Synthesis and Processing of Colloids,* 2019. https://doi.org/10.17185/duepublico/70584
26. Roper, D.K., Ahn, W., and Hoepfner, M., *J. Phys. Chem. C,* 2007, vol. 111, p. 3636.
27. Popov, A., Tikhonowski, G., Shakhov, P., Popova-Kuznetsova, E., Tselikov, G., Romanov, R., Markeev, A., Klimentov, S., and Kabashin, A., *Nanomaterials,* 2022, vol. 12, p. 1672.
28. Zhang, X., Xu, X., Li, T., Lin, M., Lin, X., Zhang, H., Sun, H., and Yang, B., *Appl. Mater. Interfaces,* 2014, vol. 6, p. 14552.
29. Dai, W., Dong, H., and Zhang, X., *Materials,* 2018, vol. 11, p. 1776.
30. Cheng, L., Liu, J., Gu, X., Gong, H., Shi, X., Liu, T., Wang, C., Wang, X., Liu, G., Xing, H., Bu, W., Sun, B., and Liu, Z., *Adv. Mater.,* 2014, vol. 26, p. 1886.
31. Kurapati, R., Muzi, L., de Garibay, A.P.R., Russier, J., Voiry, D., Vacchi, I.A., Chhowalla, M., and Bianco, A., *Adv. Funct. Mater.,* 2017, vol. 27, p. 1605176.

*Translated by D. Sventsitsky*